THE JOURNAL OF PHYSICAL CHEMISTRY C

Article

pubs.acs.org/JPCC

Clean Singlet Oxygen Production by a Re^{I} Complex Embedded in a Flexible Self-Standing Polymeric Silsesquioxane Film

Ramiro M. Spada,[†] Marjorie Cepeda-Plaza,[‡] María L. Gómez,[†] Germán Günther,[§] Pablo Jaque,[‡] Nancy Pizarro,[‡] Rodrigo E. Palacios,*[,†] and Andrés Vega*[,∥,⊥]

[†]Facultad de Ciencias Exactas Fisicoquímicas y Naturales, Departamento de Química, Campus Universitario, Universidad Nacional de Rio Cuarto y CONICET, Km 601 Ruta Nacional 36, 5800 Río Cuarto, Córdoba Argentina

[‡]Facultad de Ciencias Exactas, Departamento de Ciencias Químicas, Universidad Andres Bello, Av. República 275, 3er Piso 2531050, Viña del Mar, Chile

[§]Facultad de Ciencias Químicas y Farmacéuticas, Universidad de Chile, Sergio Livingstone 1007, Santiago, Chile

[∥]Facultad de Ciencias Exactas, Departamento de Ciencias Químicas, Universidad Andres Bello, Quillota 980 2531050, Viña del Mar, Chile

[⊥]Centro para el Desarrollo de la Nanociencia y la Nanotecnología (CEDENNA), Avda. Ecuador 3493 9170124, Santiago, Chile

Supporting Information

ABSTRACT: Rhenium complexes are versatile molecular building blocks whose tunable photophysical properties are useful in diverse opto-related applications. Herein we report the synthesis and characterization of a novel Re^{I} tricarbonyldiimine complex, [(*phen*)$Re(CO)_3Br$] (*phen*: 1,10-phenanthroline), which was found to be an efficient singlet oxygen [$O_2(^1\Delta_g)$] photosensitizer in homogeneous solution [$\Phi_{O_2(^1\Delta g)}$ = 0.55 (dichloromethane) and 0.16 (dimethylformamide)]. The photophysical properties of [(*phen*)$Re(CO)_3Br$] were thoroughly characterized in solution and modeled by means of density functional theory (DFT) and time-dependent (TD)-DFT quantum mechanical calculations. The Re complex was incorporated into a flexible polymeric silsesquioxane (SSO) film, which has excellent dopant compatibility, chemical resistance, and mechanical properties. When [(*phen*)$Re(CO)_3Br$] is embedded in the SSO film, it is found to retain most of the photophysical characteristics observed for the complex in solution. In particular, the [(*phen*)$Re(CO)_3Br$]-doped SSO films were able to photosensitize $O_2(^1\Delta_g)$ when illuminated with blue light (~405 nm). The $O_2(^1\Delta_g)$ sensitization by films in acetonitrile was followed by the photooxidation of the well-known $O_2(^1\Delta_g)$ chemical trap 9,10-dimethylanthracene (DMA) and confirmed by the direct observation of the $O_2(^1\Delta_g)$ luminescence spectrum (centered at 1270 nm) and the measurement of its kinetic profile. These results highlight the potential application of this type of polymeric material in the production of biological- or microbial-photoinactivating flexible surfaces or in the implementation of interfacial solid/liquid strategies for the photoinduced oxidation of organic compounds in solution.

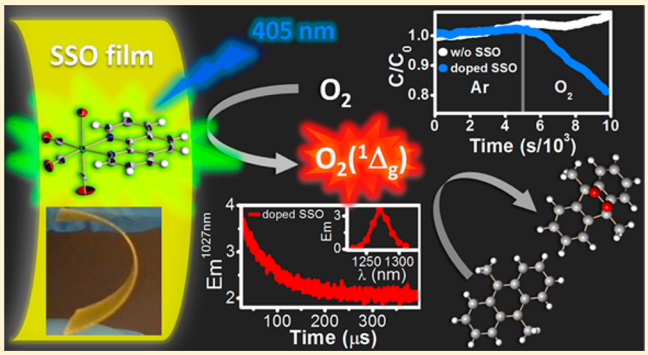

INTRODUCTION

Rhenium(I) tricarbonyldiimine complexes [(*N*,*N*)$Re(CO)_3X$] in which X is a halide are receiving considerable attention due to their interesting photophysical and photochemical properties, which can be tuned, thereby modifying the nature of the diimine ligand (*N*,*N*) or the X halide (Cl, Br).[1−3] These structural changes have a direct effect on the excited state's character.[4] Because of the above-mentioned remarkable properties, Re complexes have become very valuable molecular fragments for incorporation into molecules designed for technological applications, including light harvesting,[5] biolabeling,[6−10] sensing,[11−14] and photocatalysis,[15] and for use as emitting centers in organic light-emitting diodes (OLED).[16−19] One of the most simple chelating diimines is 1,10-phenanthroline (*phen*), which was present in the first Re^{I} tricarbonyldiimine described in early 1941.[20] Usually, rhenium diimines are widely accessible at reasonably good yields and purities by the direct reaction of the diimine with the corresponding carbonyl $Re(CO)_5X$ in an inert solvent such as benzene.[21,22] We have recently described an alternative synthesis approach involving the use of the dimeric precursor [$(CO)_3(THF)Re(\mu\text{-}Br)_2Re(THF)(CO)_3$] and softly reacting it with diphenyl-2-pyridylphosphine at room temperature to give the mononuclear complex *fac*-[*P*,*N*-{$(C_6H_5)_2(C_5H_4N)P$}$Re(CO)_3Br$] in a 61% yield.[23]

Received: February 28, 2015
Revised: April 14, 2015
Published: April 15, 2015

DOI: 10.1021/acs.jpcc.5b01990
J. Phys. Chem. C 2015, 119, 10148−10159

In addition to the intrinsic complexity of its manifold of electronic energy levels, Re complexes are of particular interest from the photochemical point of view due to their ability to generate singlet molecular oxygen, $O_2(^1\Delta_g)$, upon photoexcitation.[24]

The preparation of polymeric surfaces with $O_2(^1\Delta_g)$-sensitizing capacity is important for a number of technological applications such as the production of photoresponsive surfaces for biological inactivation or the oxidation of polyaromatic compounds. However, the inclusion of $O_2(^1\Delta_g)$ sensitizing dyes in polymeric matrices to obtain uniform dye-doped films is usually complicated by the typical heterogeneous distribution of dye across the different nanoenvironments present in the matrix. As a consequence, the energy transfer, charge transfer, oxygen permeability, and other factors relevant to the photosensitization process are modulated by a distribution of factors that are not necessarily simple; thus, the sensitizing properties of the resulting film are difficult to predict.

Silsesquioxanes (SSOs) belong to a family of hybrid organic−inorganic materials produced from the hydrolysis and polycondensation of monomers containing one organic group bridging two (or more) trialkoxysilanes or trichlorosilanes.[25−27] The organic groups covalently bound to the trialkoxysilane (or trichlorosilane) moieties can have different composition, length, rigidity, and functional groups, all of which determine the properties of the final polymeric material. One of the most-studied properties of SSO films is their capacity for emitting light in the visible range of the electromagnetic spectrum upon optical[28] or electrical[29] excitation. Strategies for tuning the photophysical and mechanical properties of SSO materials usually involve the modification of the composition of its organic bridging moieties,[30] variation of the synthesis conditions,[31] and the incorporation of nonbound matrix dopants such as organic dyes,[32] Eu^{3+},[33] and other lanthanides,[34] among others. Also, the ability of SSO films to efficiently and homogeneously disperse a large number of dopants such as Au[35,36] and Ag[37] nanoparticles, porphyrins,[38] and other organic dyes within its polymeric matrix can be tuned by introducing alkyl pendant groups. These alkyl groups not only control the dispersion of dopants but also influence the mechanical properties of the films, allowing the formation of flexible self-standing films.

Herein we investigate the photophysical and photochemical properties of [(*phen*)$Re(CO)_3Br$] in homogeneous solutions of organic solvents and uniformly incorporated into a flexible polymeric matrix composed of a bridged SSO material. Because of its excellent dopant compatibility, optical transparency, gas permeability, chemical resistance, and mechanical flexibility, the SSO film with a dodecyl pendant group was chosen as the polymer matrix to disperse the [(*phen*)$Re(CO)_3Br$] complex in this work. We found that the photophysical properties of [(*phen*)$Re(CO)_3Br$] are not significantly affected when the complex is incorporated into the polymeric matrix as compared to the properties in homogeneous solution. Experimental results were complemented with density functional theory (DFT) and time-dependent (TD)-DFT electronic structure calculations to gain a deeper understanding of the Re complex's photophysical properties. Importantly, the ability of [(*phen*)-$Re(CO)_3Br$] to photosensitize $O_2(^1\Delta_g)$ formation in a solution of organic solvents is retained upon its incorporation into the films. This latter feature highlights the potential application of this type of Re-complex-doped SSO material in the production of biological- and microbial-photoinactivating polymeric surfaces or in the implementation of interfacial solid/liquid strategies for the photoinduced oxidation of organic compounds in solution.[39−41]

EXPERIMENTAL SECTION

1. Materials. $(Re(CO)_3(THF)Br)_2$ (Sigma-Aldrich), 1,10-phenanthroline (Sigma-Aldrich), water (HPLC grade, Sintorgan), formic acid (85%, Sintorgan), dichloromethane (DCM, HPLC grade, Sintorgan), acetonitrile (MeCN, HPLC grade, Sintorgan), ethanol (EtOH, absolute grade, Cicarelli), dimethylformamide (DMF, spectroscopic grade, Uvasol, Merck), methanol (MeOH, spectroscopic grade, Uvasol, Merck), quinine sulfate (99%, Sigma-Aldrich), perinaphthenone (99%, Sigma-Aldrich), sulfuric acid (H_2SO_4, 98%, EMSURE, Merck), 9,10-dimethylanthracene (DMA, 99%, Sigma-Aldrich), dodecylamine (DAM, 98%, Fluka), and glycidoxypropyltrimethoxysilane (GPTMS, 97%, Sigma-Aldrich) were used as received. The toluene (analysis grade, EMSURE, Merck), DCM (analysis grade, EMSURE, Merck), and hexane (analysis grade, EMSURE, Merck) used for synthesis and recrystallization were dried according to standard procedures and freshly distilled before use. Standard Schlenck techniques were employed for all manipulations. Tetrahydrofuran (THF) (HPLC grade, Cicarelli) was refluxed for 5 h with potassium hydroxide pellets (KOH, pro analysis grade, Taurus) and subsequently distilled and stored over freshly activated molecular sieves (4 Å, Aldrich). Argon (Ar, 99.99%, Air Liquide) and oxygen (O_2, 99%, Air Liquide) were used as received.

2. Rhenium Complex Synthesis. The complex [(*phen*)-$Re(CO)_3Br$] was prepared by the direct reaction of $(Re(CO)_3(THF)Br)_2$ and 1,10-phenanthroline in a 1:1 stoichiometric relation at room temperature according to what is depicted in Scheme 1. A colorless solution of 202 mg of the

Scheme 1

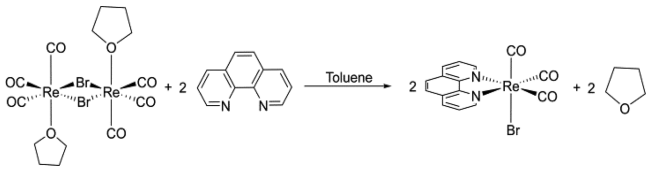

ligand (1.12 mmol) in toluene was added dropwise to a colorless solution of 475 mg (0.562 mmol) of $(Re(CO)_3Br(THF))_2$ dissolved in 20 mL of toluene. After the addition was completed, 20 mL of toluene was then added. The mixture was reacted overnight with stirring at room temperature. The toluene was then removed from the reaction mixture by evaporation at reduced pressure, yielding a crude yellow material. Crystals (X-ray diffraction quality) were obtained after recrystallization in a DCM/hexane mixture (yield of 535 mg, 90%).

Elemental Analysis. Calculations for $C_{15}H_8BrN_2O_3Re$: C, 33.97%; H, 1.52%; N, 5.28%. Found: C, 33.60%; H, 1.90%; N, 5.61%. Elemental analyses were obtained from Centro de Análisis Pontificia Universidad Católica de Chile.

IR Spectroscopy (cm^{-1}). 1930 (s), 1905 (s), 2017 (s), 1654 (w), 1560 (w), 1425 (w).

X-ray Diffraction. The crystal structure of *fac*-[(*phen*)Re-$(CO)_3Br$] at 273 K was determined by X-ray diffraction on a plate-shaped 0.10 × 0.10 × 0.05 mm^3 yellow single crystal. Data

DOI: 10.1021/acs.jpcc.5b01990
J. Phys. Chem. C 2015, 119, 10148−10159

a.-

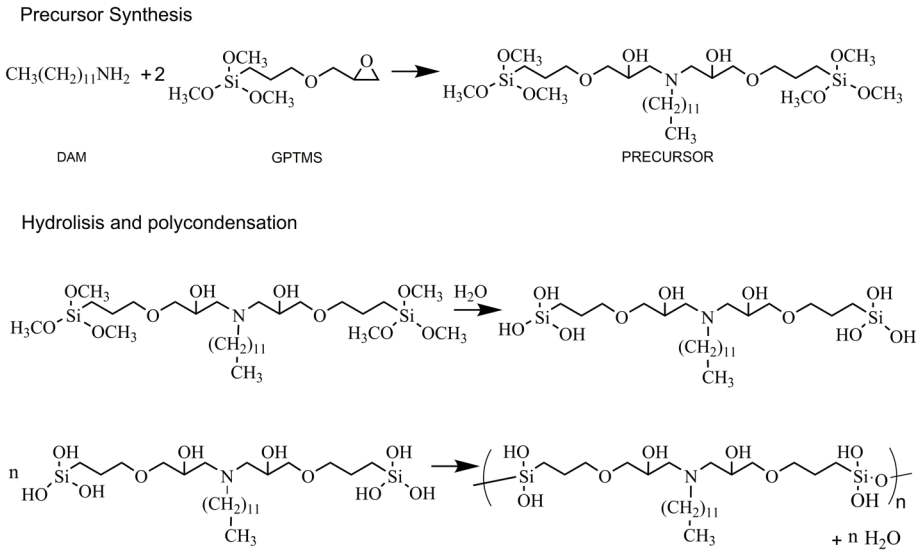

b.-

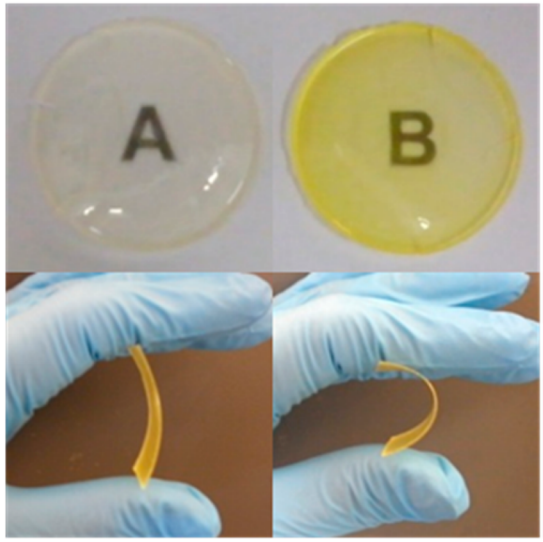

Figure 1. a. Schematic representation of film synthesis. **b.** Photograph of neat (upper left) and [(*phen*)Re(CO)$_3$Br]-doped (upper right) SSO films. Doped SSO film before (lower left) and after (lower right) bending.

collection was done on a SMART APEX II CCD diffractometer system. Data were reduced using SAINT,[42] and the structure was solved by direct methods, completed by difference Fourier synthesis, and refined by the least-squares method using SHELXL.[43] Multiscan absorption corrections were applied using SADABS.[44] The hydrogen atoms' positions were calculated after each cycle of refinement with SHELXL using a riding model for each structure with a C−H distance of 0.95 Å. The U_{iso}(H) values were set equal to 1.2U_{eq} of the parent carbon atom.

3. Films Preparation. The synthesis of the SSO polymeric matrix has been reported before.[35] The silane precursor, containing a dodecyl pendant chain, was synthesized by employing stoichiometric amounts of DAM and GPTMS in THF as shown in Figure 1a. The reaction mixture was held at 58 °C for 48 h in a nitrogen atmosphere until the complete conversion of the precursor was attained. The films were obtained by a sol−gel polycondensation process in which the precursor silane was hydrolyzed by adding water and a small amount of formic acid (used as a catalyst). The low content of acid yields a relatively slow polycondensation rate, allowing the dodecyl pendant group to become sufficiently accommodated in the matrix to obtain flexible self-standing films (see Figure 1b, down). For undoped films, the prepolymeric solution was prepared by mixing a 0.1 mol·L^{-1} solution of precursor in THF with the appropriate amount of catalyst and water to achieve a molar ratio of 1:0.1:3 (Si\HCOOH\H_2O). Doped films were prepared by the addition of 2.12 mg of [(*phen*)Re(CO)$_3$Br] to the prepolymeric mixture. In all cases, samples of 25 mL of prepolymeric solution were cast in polyacetal containers (5 cm in diameter and 3 cm in height) covered with aluminum foil to reduce the rate of solvent evaporation. Containers were placed in a natural convection flow oven at 308 K for 24 h. After this period, colorless and light-yellow films were obtained for neat

DOI: 10.1021/acs.jpcc.5b01990
J. Phys. Chem. C 2015, 119, 10148−10159

and [(*phen*)Re(CO)$_3$Br]-doped materials, respectively (see Figure 1b, top). The resulting films were ∼500 μm in thickness, mechanically flexible (see Figure 1b, bottom), and easily detachable from the polyacetal mold.

4. Photophysical Measurements and Procedures. *Steady-State Absorption.* The UV−vis absorption spectra of [(*phen*)Re(CO)$_3$Br] in solution were recorded on an Agilent 8453 diode-array spectrophotometer in the range of 250−800 nm in aerated DCM or DMF solutions. The molar absorptivity was determined according to the Lambert−Beer law by measuring the absorbance at 385 nm (DCM) and at 375 nm (DMF) for different concentrations of [(*phen*)Re(CO)$_3$Br] solutions ranging from 1 to 20 μM. The absorption spectra of the SSO films doped with [(*phen*)Re(CO)$_3$Br] were obtained in a Shimadzu UV-IR 2041 absorption spectrophotometer equipped with an integrating sphere module (Shimadzu ISR-2200) to reduce the scattering effects of the solid matrix on the absorption spectra.

Steady-State Emission. The emission spectra of [(*phen*)Re(CO)$_3$Br] in solution were recorded with a Horiba Jobin Yvon FluoroMax-4 spectrofluorometer in DCM and DMF at room temperature or in EtOH/MeOH glass (4:1, v/v) at 77 K. The quantum yields of luminescence were measured at room temperature using quinine sulfate in 0.1 mol·L^{-1} H_2SO_4 (quantum yield (Φ_{em}) = 0.546 for excitation at 350 nm)[45] as the actinometer. Other solvents, such as MeCN and EtOH, were also employed to observe the solvent polarity effect. The emission from film samples was measured using a solid sample holder placed 45° from the excitation beam.

Time-Resolved Emission. Luminescence decay curves were recorded using the time-correlated single photon counting technique in a PicoQuant FluoTime 300 fluorescence lifetime spectrometer. An LDH-P-C-405 laser was employed as the pulsed light source (full width at half maximum of ∼54 ps; pulse energy of 31 pJ). Singlet oxygen emission experiments were performed using the instrument "burst" mode, consisting of a train of laser pulses at a high (MHz) repetition rate initially emitted (rather than a single pulse) and then switched off to detect the emission of the sample. The individual laser pulses act like a single long pulse with a much higher energy. The generation of singlet oxygen was monitored at 1270 nm using a Hamamatsu NIR-PMT detector (H10330-45). The solutions were air-equilibrated or either oxygen- or argon-saturated. To carry out the measurements with [(*phen*)Re(CO)$_3$Br]-doped and neat SSO films under oxygen-free conditions, we sealed the samples at high vacuum (1×10^{-5} mmHg) using the freeze−thaw procedure. Quantum yields of singlet oxygen generation were measured at room temperature using perinaphthenone as the actinometer (Φ_Δ = 0.95 in DCM).[46] Singlet oxygen emission spectra were reconstructed by recording individual emission decays acquired at 10 nm intervals in the 1220−1310 nm range for samples under the same experimental conditions. The decay traces were globally fitted using FluoFit software, and the fitted intensities at t = 0 for each decay were used to reconstruct the $O_2(^1\Delta_g)$ emission spectra.

Rate Constant Calculations. Radiative (k_r) and nonradiative (k_{nr}) rate constants were calculated from the emission quantum yield (Φ_{em}) and the luminescence lifetimes (τ), assuming that the intersystem crossing yield is unity:

$$k_r = \Phi_{em}/\tau \quad (1)$$

$$\tau = (k_r + k_{nr})^{-1} \quad (2)$$

The intrinsic lifetime corresponds to the lifetime of the radiative decay:

$$\tau_{intr} = 1/k_r \quad (3)$$

The bimolecular quenching rate constant by O_2, k_q, was estimated using eq 4

$$\tau^{-1} = \tau_o^{-1} + k_q[O_2] \quad (4)$$

where τ_o and τ are the lifetimes in the absence or the presence of oxygen, respectively. Oxygen concentrations were assumed to be 2.28 and 2.42 mM in air-saturated DCM and DMF solutions.[47]

Photooxidation of 9,10-Dimethylanthracene (DMA). Photo-oxidation experiments were conducted by submerging the film in a DMA solution in MeCN inside a fluorescence cuvette. It is well known that DMA reacts efficiently with $O_2(^1\Delta_g)$ (k_T^{DMA} = 8.8 × 10^7 [M^{-1} s^{-1}]) to form the DMA endoperoxide (DMA−O_2).[48] The [(*phen*)Re(CO)$_3$Br]-doped SSO film was irradiated with two blue LEDs (λ center emission of ∼467 nm, full width at half maximum of ∼28 nm, and a total optical power of ∼14 mW) while the absorbance of DMA in MeCN as a function of time was simultaneously monitored. The absorption spectra of the DMA solution were automatically collected at constant time intervals using a UV−vis absorption spectrophotometer (HP 8452A, Hewlett-Packard) equipped with a kinetic software module. Special care was taken to avoid obstruction of the spectrophotometer optical path by the film. The extinction coefficient of the peroxide DMA−O_2 in MeCN at 377 nm ($\varepsilon_{DMA-O_2}^{377}$ < 10 [M^{-1} cm^{-1}]) is negligible compared to that of DMA under the same conditions (ε_{DMA}^{377} ≈ 10 000 [M^{-1} cm^{-1}]).[49] Thus, the oxidation reaction (DMA + $O_2(^1\Delta_g)$ → DMA−O_2) is conveniently followed by monitoring changes in absorption at 377 nm and directly assigning these changes to variations in DMA concentration. Kinetic traces were constructed by monitoring the absorption at 377 nm as a function of time. Each absorption value was first corrected by variations in lamp intensity over time (as monitored in the ∼780−800 nm region where the sample does not absorb), and the resulting values were later normalized to the absorption at t = 0 s (t_0) to yield C and C_0 values, which correspond to the concentration of DMA at any time (t) and at t_0, respectively. During measurements, the solutions were continuously purged with either Ar or O_2. Both gases were previously saturated with MeCN to reduce solvent evaporation in the reaction cuvette.

5. Computational Methods. All calculations reported here were performed with the Gaussian 09 package (revision C.1).[50] The molecular geometry optimizations of [(*phen*)Re(CO)$_3$Br] in both the ground state and the lowest-lying triplet excited state were performed using the hybrid-type B3LYP[51,52] exchange−correlation functional combined with the split-valence double-ζ basis set augmented with d-type polarization and diffuse functions for carbon, oxygen, nitrogen, and bromine and the p-type polarization functions for hydrogen atoms, i.e., the standard 6-31+G(d,p) basis set for the ligands. The rhenium core electrons were described by an effective core potential that replaces the 60 inner electrons with a relativistic pseudopotential developed by Hay and Wadt[53] (the so-called LANL); the valence electrons were quantum mechanically treated with the respective optimized valence (8s6p3d)/[3s3p2d] basis set, i.e., LANL2DZ. To confirm that the geometries were minimal on the potential energy surface, we carried out a vibrational analysis. The TD-DFT calculations

DOI: 10.1021/acs.jpcc.5b01990
J. Phys. Chem. C 2015, 119, 10148−10159

were performed in solution using DCM and DMF as solvents to obtain both of the vertical excitation transition energies for several singlet excited states and the emission features; the solute−solvent interactions were described by the polarizable continuum model (PCM)[54] in nonequilibrium solvation protocols as implemented in Gaussian 09, whereas the emission was studied from the triplet excited state using equilibrium solvation protocols. The cavity was created using the default, i.e., the united-atom universal force field (UFF) topological model of atomic radii.

RESULTS AND DISCUSSION

1. Structural Description. The [(*phen*)Re(CO)$_3$Br] complex has a central Re^I ion with an octahedral coordination environment, completed by three carbonyl groups in a *fac* correlation, a bidentate phenanthroline, and a bromide, as shown in Figure 2. The molecule has a mirror plane (crystallographic) passing across Re, Br, C7, and O7, and its point symmetry group is C_s. Table 1 shows the main bond distances and angles.

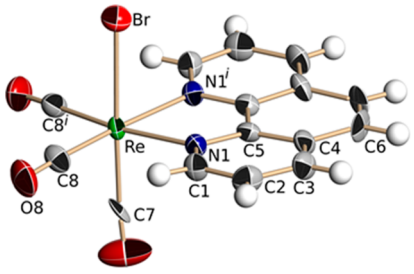

Figure 2. Molecular structure diagram for [(*phen*)Re(CO)$_3$Br] showing the atom-numbering scheme. Displacement ellipsoids are drawn at the 50% level of probability. Symmetry equivalent ^{i}: $x, -y, z$.

Table 1. Bond Distances (Å) and Angles (deg) for *fac*-[(*phen*)Re(CO)$_3$Br] Calculated from Crystallographic Data[a]

Re−N1	2.196 (10)	Re−Br	2.617 (2)
Re−C7	1.972 (18)	Re−C8	1.930 (14)
N1−Re−Br	85.2 (3)	C8−Re−N1	95.8 (5)
C8^i−Re−N1	171.9 (5)	C8−Re−C7	89.0 (5)
C8−Re−Br	92.3 (4)	C7−Re−N1	93.3 (4)

[a]Symmetry code: $^1x, -y, z$.

2. Spectroscopic Properties. *Absorption Spectra.* The absorption spectra of [(*phen*)Re(CO)$_3$Br] in DCM and DMF are shown in Figure 3a. The lowest-energy absorption band of the Re^I complex is broad in both solvents and appears in the near-UV region ($\varepsilon_{DCM}^{385} = 10.2 \times 10^3$ [M^{-1}cm^{-1}] in DCM; $\varepsilon_{DMF}^{375} = 6.1 \times 10^3$ [M^{-1}cm^{-1}] in DMF). The hypsochromic shift of this absorption band as the solvent polarity is increased from DCM to DMF is compatible with the typical assignation involving a metal-to-ligand charge transfer (MLCT) transition.[55] The absorption band with a shoulder at a higher energy ($\varepsilon_{DCM}^{268} = 80.8 \times 10^3$ [M^{-1} cm^{-1}] in DCM; $\varepsilon_{DCM}^{277} = 46.7 \times 10^3$ [M^{-1} cm^{-1}] in DMF) is assigned to the ligand-centered (LC) absorption corresponding to the $\pi\pi^*$ transition of phenanthroline, being consistent with the band shape, position, and molar extinction coefficients reported in the literature.[56,57] The absorption spectra of [(*phen*)Re(CO)$_3$Br]-doped and neat SSO films are shown in Figure 3b. There is an important overlap between the absorption of the SSO matrix and of

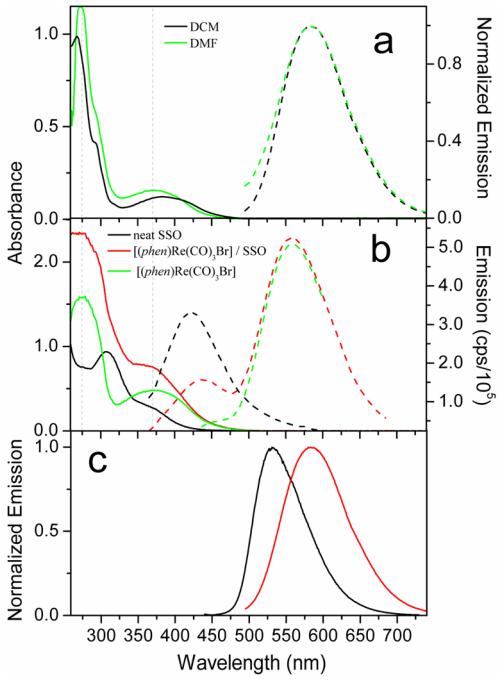

Figure 3. a. Absorption (solid lines) and emission (dashed lines) spectra of [(*phen*)Re(CO)$_3$Br] in DCM (black lines) and DMF (green lines) solutions. Emission spectra were collected with excitation at 384 nm. The [(*phen*)Re(CO)$_3$Br] concentration was 1.2×10^{-5} M for all samples. **b.** Absorption (solid lines) and emission (dashed lines) spectra of [(*phen*)Re(CO)$_3$Br] on doped (red line) and neat (black line) SSO films. The green spectra were constructed by subtracting the absorption (emission) of the neat SSO film (black line) from the absorption (emission) of the [(*phen*)Re(CO)$_3$Br]-doped SSO film (red line). Emission spectra were collected with excitation at 350 nm. **c.** Emission spectra of [(*phen*)Re(CO)$_3$Br] in DCM at room temperature (red line) and in 4:1 ethanol/methanol glass at 77 K (black line).

[(*phen*)Re(CO)$_3$Br]; thus, the intrinsic absorption of the Re^I complex in the polymeric matrix (green line) was estimated by subtracting the neat film absorption from that of the [(*phen*)Re(CO)$_3$Br]-doped film. The resulting spectrum is very similar to that of [(*phen*)Re(CO)$_3$Br] in DMF solution (with well-defined peaks at 273 and 374 nm), albeit with broader bands associated with the heterogeneity of the nanoenvironments present in the film. This result proposes that the Re^I complex inside the SSO matrix senses, on average, a polarity comparable to that of DMF and suggests a significant stabilizing interaction between [(*phen*)Re(CO)$_3$Br] and the polymeric matrix, confirming the excellent dopant compatibility of the SSO film. No evidence of Re complex aggregates is observed in the absorption spectra, consistent with the homogeneous distribution of dopant seen in pictures of the film (see Figure 1b).

Steady-State Emission. The [(*phen*)Re(CO)$_3$Br] complex showed a broad and structureless emission band centered at around 585 nm (in DMF) and 583 nm (in DCM) at room temperature after excitation at 384 nm (Figure 3a, dashed lines). The maximum in the emission band was independent of the excitation wavelength, confirming that the predominant emissive excited state of the Re^I complex has MLCT characteristics. Triplet character can be attributed to this excited state due to the ultrafast intersystem crossing reported for these kinds of Re^I diimine complexes.[58]

DOI: 10.1021/acs.jpcc.5b01990
J. Phys. Chem. C 2015, 119, 10148−10159

Table 2. Summary of the Photophysical Properties of [(*phen*)Re(CO)$_3$Br] in Solution[a]

solvent	λ_{abs}/nm	λ_{em}/nm	Φ_{em}	τ/ns	k_r /(10^4 s^{-1})	k_{nr} /(10^6 s^{-1})	τ_{intr}/μs	k_q /(10^9 M^{-1} s^{-1})	Φ_Δ
DCM	385 (10200)	583						1.27	
Ar			0.0196	508.9	3.85	1.93	26.0		
air			0.0108	205.8	5.25	4.81	19.0		0.55
O_2				68.0					
DMF	375 (6100)	585						2.65	
Ar			0.0106	298.9	3.55	3.31	28.2		
air			0.0046	102.4	4.49	9.72	22.3		0.16
O_2				28.5					

[a]Errors were lower than 10%.

The emission quantum yield values were dependent upon the solvent polarity being higher in DCM (Φ_{em} = 10.8 ± [0.7 × 10^{-3}], similar to the value reported previously by Si et al.[59]) than that measured in DMF (Φ_{em}= 4.6 ± [0.2 × 10^{-3}]), as is usually found for these kinds of complexes.[60] Because the k_r values are very similar for both solvents (see Table 2), the Φ_{em} decrease when going from DCM to DMF can be directly associated with a k_{nr} rise with increasing solvent polarity. Analogous behavior has been previously reported for ruthenium 2,2′-bipyridine complexes ($[Ru(bpy)_3]^{2+}$) and rationalized by invoking the energy gap law (EGL) for radiationless transitions, given the significant emission energy decrease with increasing solvent polarity also observed for these Ru complexes.[61] However, the lack of significant dependence of the [(*phen*)Re(CO)$_3$Br] emission energy on the solvent polarity indicates that other factors must be at play in determining the strong solvent polarity effect observed for k_{nr} and the insignificant effect observed for k_r in our systems. These factors might include larger spin−orbit coupling effects for metals of the third row or specific solvent−metal interactions that affect the vibrational relaxation processes.[62] In fact, for Re^I tricarbonyl complexes, the significant dependence of the MLCT excited-state relaxation on the ν_{Re-C} and ν_{CO} vibrations is the main reason for the observed differential solvatochromic behavior of Re complexes as compared to that of Ru complexes.[1] The CO stretching mode is able to act as a vibrational acceptor of the excited-state energy; this ability is in part responsible for the smaller dipole moment of the excited molecule, which in turn makes the energy of the emission less sensitive to solvent polarity (the emission spectra in DCM and DMF are almost identical).[63]

The emission measurements of [(*phen*)Re(CO)$_3$Br] in EtOH/MeOH glass at low temperature (77 K) showed that the emission maximum is shifted to higher energies as compared to that of the spectrum at room temperature (Figure 3c). This hypsochromic shift, a phenomenon also called the "rigidochromic effect",[64] is associated with the restricted movement in the microenvironment surrounding [(*phen*)Re(CO)$_3$Br] within the frozen glass as compared to the relatively facile rearrangement of solvent molecules at room temperature in such a way that both the solute and the solvent relax to reach a new equilibrium condition. Thus, the unrestricted solvent movement in solution allows the stabilization of the excited-state molecular configuration and lowers the energy of the electronic transition corresponding to the emission process. The structureless emission band at low temperature supports the assignation of the MLCT character to the observed transition.[21,65]

The emission spectrum of a [(*phen*)Re(CO)$_3$Br]-doped SSO film excited at 350 nm shows two broad and structureless emission bands centered at 558 and 422 nm corresponding to [(*phen*)Re(CO)$_3$Br] and SSO emission, respectively (see Figure 3b, red dashed line). The intrinsic emission of the Re^I complex into the polymeric matrix (Figure 3b, green dashed line) was estimated by subtracting the neat film emission (black dashed line) scaled by an arbitrary factor from that of the [(*phen*)Re(CO)$_3$Br]-doped film (red dashed line). The similarity of the resulting spectrum for the complex into the film (Figure 3b, green dashed line) to that observed for [(*phen*)Re(CO)$_3$Br] at low temperature (Figure 3c, black line) indicates a rigid surrounding nanoenvironment (no evidence of aggregation), which prevents the molecular relaxation within these sites in the polymer matrix (significant hypsochromic shift).

Time-Resolved Emission. The luminescence of the aerated solutions of the Re^I complex followed single-exponential decay curves after the pulsed excitation at 405 nm (Figure 4a), and its emission lifetime was influenced by the polarity of the solvent: as the solvent polarity increases, lifetime values diminish (Table 2). This is the typical behavior shown for Re^I complexes with a dominant triplet MLCT excited state; however, the contribution of other emissive excited states (e.g., ligand-centered) cannot be discarded.[60]

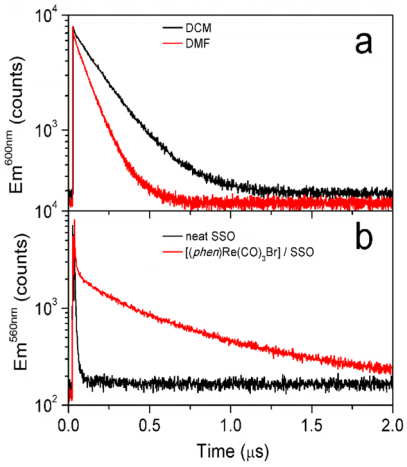

Figure 4. Luminescence decay curves of [(*phen*)Re(CO)$_3$Br] **a.** in DCM (black line) and DMF (red line) solutions and **b.** on doped (red line) and neat (black line) SSO films. Emission decay curves were collected at room temperature after excitation at 405 nm.

Table 2, which summarizes the main photophysical parameters of [(*phen*)Re(CO)$_3$Br] in homogeneous solutions, shows that k_{nr} is the only parameter that significantly depends on the polarity of the solvent. This dependence, typically found for the MLCT excited states, could be explained by invoking

DOI: 10.1021/acs.jpcc.5b01990
J. Phys. Chem. C 2015, 119, 10148−10159

expressions for the EGL.[66] In particular, the dependence on the classical solvent vibrational trapping energy term (χ_0) seems to play an important role in the tricarbonyl Re^I complexes.[1] We postulate that the CO bond present in DMF may act as a vibrational acceptor (in an analogous way to the CO ligands in [(*phen*)$Re(CO)_3Br$]) promoting the nonradiative decay, therefore lowering the emission quantum yield and lifetime as compared to the same properties in DCM. The radiative lifetime (τ_{intr}), on the order of 20 μs, further supports the assignment of the MLCT character to the involved transition, as ligand-centered phosphorescence and fluorescence emission usually have longer and shorter lifetimes, respectively.[67] The incorporation of [(*phen*)$Re(CO)_3Br$] into the polymeric film resulted in changes in its luminescence lifetime compared to the values measured in homogeneous solvents. Time-resolved luminescence traces of [(*phen*)$Re(CO)_3Br$]-doped SSO films were fitted with a biexponential model, and the resulting parameters are summarized in Table 3.

Table 3. Luminescent Lifetimes of [(*phen*)$Re(CO)_3Br$] in SSO Films[a]

media	$\tau_1/\mu s$	$\tau_2/\mu s$
Re^I–SSO film, air	0.230 (57%)	0.850 (43%)
Re^I–SSO film, degassed	0.284 (67%)	1.065 (33%)
Re^I–SSO film, air (MeCN)	0.109 (77%)	0.416 (23%)
Re^I–SSO film, degassed (MeCN)	0.100 (75%)	0.428 (25%)

[a]Excitation and emission wavelengths are 405 and 560 nm, respectively. Errors were lower than 10%. Values in parentheses are amplitudes in percent contribution from each decay component.

Figure 4b shows the time-resolved luminescence intensities recorded at 560 nm for Re-complex-doped (red line) and neat (black line) films after excitation at 405 nm in the absence of oxygen. As expected for solid media, biexponential decays were found to have longer lifetime values than those measured in homogeneous media.[3,68] Rigorous analysis of time-resolved emission data in a nonhomogeneous system (such as the SSO polymer matrix) requires the use of a distribution of exponential decays to describe the kinetics of the emissive states. This distribution of decays accounts for the distribution of available environments into the polymer matrix, even in the absence of quenchers such as oxygen or the solvent. In our analysis, we needed a minimum of two exponential components to adequately fit the experimental data within the experimental error. However, it is likely that this pair of decay components corresponds to a weighted mean value of the actual distribution of decays associated with the emissive species in different nanoenvironments. In a simplified view, the existence of two emission components, τ_1 and τ_2, could be attributed to significantly different locations of the [(*phen*)$Re(CO)_3Br$] molecules within the polymer film. For the dry film, the longest-lived component (τ_2) can, in principle, be associated with the [(*phen*)$Re(CO)_3Br$] molecules deep inside the polymer film, where the dynamic quenching by diffusing O_2 and the penetration of solvent molecules are significantly restricted. Alternatively, the existence of two emission components for the dry film can be related to the location-dependent matrix–[(*phen*)$Re(CO)_3Br$] interactions. For the film submerged in MeCN, the short component ($\tau_1 \approx 0.1$ μs) correlates well with the excited-state lifetime of the [(*phen*)-$Re(CO)_3Br$] dissolved in MeCN ($\tau_{MeCN} = 0.07$ μs); thus, we associate this component, τ_2, with complex molecules near the film–solvent interface where [(*phen*)$Re(CO)_3Br$]–solvent interactions are likely to occur. Surprisingly, we found that [(*phen*)$Re(CO)_3Br$] is highly photostable when we worked in solution or on a doped SSO film, and no evidence of photodegradation was observed after our measurements. Moreover, leakage of the rhenium complex from the SSO matrix was not observed when the doped film was submerged in organic solvent for more than 24 h.

Emission Quenching by Oxygen. Figure 5a shows the luminescence of [(*phen*)$Re(CO)_3Br$] in DCM at room

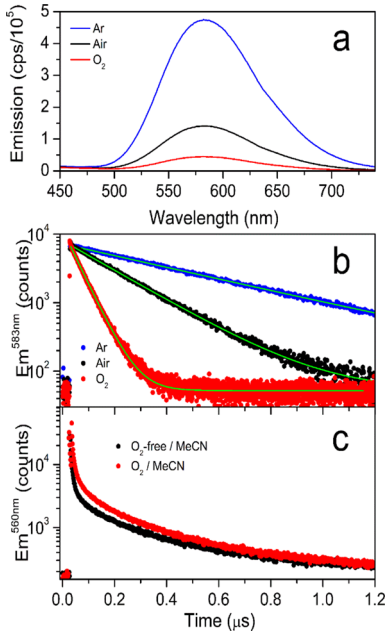

Figure 5. a. Dissolved-oxygen-dependent emission of [(*phen*)$Re(CO)_3Br$] in DCM. **b.** Dissolved-oxygen-dependent luminescence decay curves of [(*phen*)$Re(CO)_3Br$] in DCM: air-equilibrated solution (black line), O_2-saturated solution (red line), and Ar-saturated solution (green line). **c.** Luminescence decay curves of [(*phen*)$Re(CO)_3Br$]-doped SSO films immersed in air-equilibrated MeCN (red line) and oxygen-free MeCN solution (black line). Luminescence decays were collected after excitation at 405 nm.

temperature as a function of the O_2 concentration (partial pressure) in solution. The data indicate that [(*phen*)$Re(CO)_3Br$] emission is sensitive to the presence of oxygen, being ~90% quenched in solutions saturated with O_2 relative to the emission of solutions saturated with Ar. Time-resolved luminescence measurements in solution (see Figure 5b) are consistent with the steady-state results, indicating strong dynamic quenching in air-equilibrated solutions relative to the emission in argon-saturated solutions. Contrary to the behavior observed in homogeneous solvents, the presence of oxygen does not seem to significantly affect the [(*phen*)$Re(CO)_3Br$] emission lifetime values of the doped film immersed in MeCN (see Figure 5c). This result is rationalized, considering that the quenching of the fraction of [(*phen*)$Re(CO)_3Br$] embedded in the film that is accessible to O_2 occurs on a time scale much shorter than that shown in Figure 5c.

However, the [(*phen*)$Re(CO)_3Br$] emission lifetimes were significantly affected when the doped film was immersed in MeCN, showing similar lifetime values to those obtained in a polar solvent such as DMF. We rationalize this phenomenon as mainly a consequence of the solvent-induced swelling of the

DOI: 10.1021/acs.jpcc.5b01990
J. Phys. Chem. C 2015, 119, 10148–10159

Table 4. Summary of the First Four Lower-Lying Calculated Transitions of [(*phen*)Re(CO)$_3$Br] in DCM and DMF

solvent	λ (nm)	E (eV)	f	main components
DCM	439	2.82	0.0011	H → L (99%)
	422	2.94	0.0527	H-1 → L (97%)
	395	3.14	0.0144	H-1 → L + 1 (99%)
	328	3.78	0.0441	H-6 → L + 1 (4%), H-4 → L + 2 (−5%), H-3 → L (89%)
DMF	424	2.93	0.0011	H → L (99%)
	408	3.04	0.0587	H-1 → L (97%)
	381	3.26	0.0163	H-1 → L + 1 (97%)
	325	3.82	0.0325	H-6 → L + 1 (3%) H-4 → L + 2 (−6%) H-3 → L (89%)

polymeric film, which facilitates both the solvent and the O_2 interactions with the embedded [(*phen*)Re(CO)$_3$Br] molecules.

The significant quenching of the [(*phen*)Re(CO)$_3$Br] emission by the presence of oxygen indicates significant triplet character of the MLCT excited state and suggests the efficient photosensitization of $O_2(^1\Delta_g)$ by the Re complex (see Table 2).

3. Quantum Mechanical Calculations. Quantum mechanical calculations were performed to gain a better understanding of the Re^I complex photophysical properties, complementing the experimental data. DFT calculations were used to optimize the geometry of [(*phen*)Re(CO)$_3$Br] in both the ground singlet state and the excited triplet state. Computed bond distances and angles for the optimized geometry of [(*phen*)Re(CO)$_3$Br] in the ground state (Table S1 in Supporting Information) are within 0.050 Å and 1.2° of those found in the X-ray crystal structure (Table 1). The optimized geometry for the low-lying triplet excited state (Table S1 in the Supporting Information) shows a slightly deformed conformation compared to that of the ground singlet state. This avoids an imaginary frequency as otherwise exhibited by the C_s structure. The structural deformations occurring upon the transition from the ground state to the relaxed excited triplet state are small; in particular, the Re−N and Re−Br distances are slightly shortened, and the Re−C distances are slightly elongated (consistent with the MLCT character of the transition).

TD-DFT calculations were performed to gain insights into the origins of the lowest-energy absorption bands of [(*phen*)Re(CO)$_3$Br] in solution, which are then associated with the electronic transitions responsible for the observed luminescence. The first four lower-lying calculated transitions with nonzero oscillator strengths (f) in both DCM and DMF are shown in Table 4. It can be noted that the calculated lowest-energy singlet excited state is almost entirely composed of HOMO → LUMO (H → L) excitation, and the following two singlet excited states are mainly composed of H-1 → L and H-1 → L + 1 excitation. Figure 6 displays an energy-level diagram together with the contour maps of the molecular orbitals involved in the lower-lying vertical excitation transitions as a function of the solvent polarity. On the basis of the contour maps and the composition of the two higher occupied and lower unoccupied molecular orbitals for the Re^I complex, it was concluded that these transitions have mixed metal-to-ligand and ligand-centered character, i.e., [dπ(Re) + p(Br) → π^*(*phen*)]. From the analogous calculations, it is also possible to assign the higher-energy absorption band to a ligand-centered transition $\pi\pi^*$ (data not shown). The calculations show the stabilization of H-1 and H by 0.07 eV and the destabilization of L and L + 1 by 0.03 and 0.07 eV, respectively, as the solvent polarity

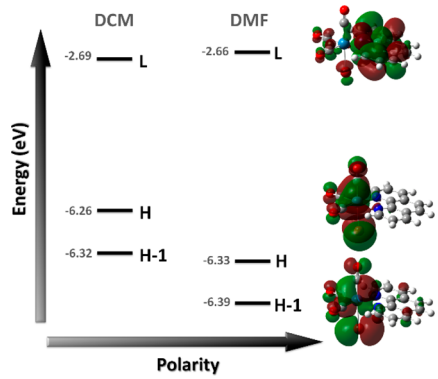

Figure 6. Schematic energy-level diagram and contour maps of selected molecular orbitals (H-1, H, L, and L + 1) for [(*phen*)Re(CO)$_3$Br] as a function of the solvent polarity computed at the PCM/B3LYP/LANL2DZ/6-31+G(d,p) level of theory.

increases. These results are in qualitative agreement with the experimental blue shift observed for the lowest absorption band when going from DCM to DMF. Analogous qualitative agreement with the experimental data is seen for the two lower-lying emission transitions (see Table S3 in Supporting Information).

Interestingly, transition-energy values calculated by TD-DFT are in better agreement with the experimental data than those calculated from the energy difference between the triplet excited state and the ground singlet states ($\Delta E_{T\text{-}S0}$: 2.55 eV/486 nm and 2.60 eV/478 nm for DCM and DMF, respectively). Notice that the triplet excited state is 0.05 eV more stable in DMF than in DCM. On the basis of the calculated oscillator strength (f), the main emission transitions came by L → H and L → H-1 emission, which are thus assigned as a [dπ(Re(CO)$_3$) + p(Br) + π(*phen*) → π^*(*phen*)] transition with mixed MLCT and LCCT character, as can be seen from the percent composition of the molecular orbitals compiled in Table S4 of the Supporting Information.

4. Photosensitized Generation of Singlet Oxygen $O_2(^1\Delta_g)$. *Singlet Oxygen Emission.* To explore the ability of [(*phen*)Re(CO)$_3$Br] to photosensitize the formation of singlet oxygen, we carried out experiments measuring its characteristic emission at 1270 nm. The near-infrared transient signals were detected after excitation of [(*phen*)Re(CO)$_3$Br] at 405 nm in DCM, DMF, and MeCN (air-equilibrated solutions). Figure 7a shows the emission decay recorded in MeCN. Time-resolved luminescence intensity traces acquired at 1270 nm were fitted to single-exponential decays with lifetimes of 89.8, 23.3, and 78.0 μs in DCM, DMF, and MeCN, respectively. The agreement of the measured values with those reported in the literature for $O_2(^1\Delta_g)$[69] confirms the assignment of the observed signal to this molecular oxygen species. Additionally,

DOI: 10.1021/acs.jpcc.5b01990
J. Phys. Chem. C 2015, 119, 10148−10159

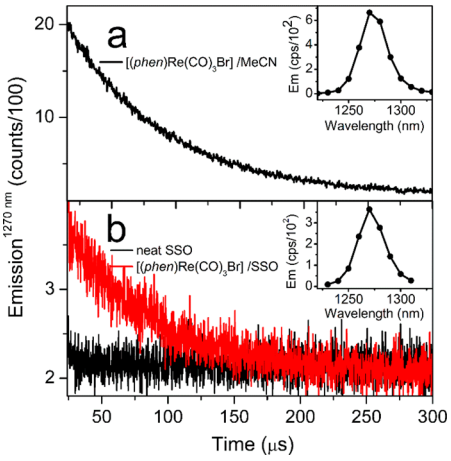

Figure 7. a. Luminescence decay of the $O_2(^1\Delta_g)$ generated by [(*phen*)Re(CO)$_3$Br] in MeCN. The inset shows the sensitized $O_2(^1\Delta_g)$ emission spectrum in MeCN. **b.** Luminescence decay of the $O_2(^1\Delta_g)$ generated by [(*phen*)Re(CO)$_3$Br]-doped (red line) and neat (black line) SSO films in MeCN. The inset shows the sensitized $O_2(^1\Delta_g)$ emission spectrum generated by the [(*phen*)Re(CO)$_3$Br]-doped film in MeCN. Luminescence decays were collected after excitation at 405 nm.

the characteristic emission spectrum of $O_2(^1\Delta_g)$ centered at 1270 nm was measured in MeCN, and it is shown in the Figure 7a inset. Using perinaphthenone as the standard, we calculated the measured $O_2(^1\Delta_g)$ generation quantum yields as 0.55 and 0.16 for DCM and DMF, respectively, revealing a sensitivity to solvent polarity. Similar values have been reported for other Re^I complexes.[70,71] Importantly, evidence for singlet oxygen generation was found after irradiation at 405 nm of the [(*phen*)Re(CO)$_3$Br]-embedded SSO film immersed in MeCN.

The relatively long-lived (τ = 65 μs) transient emission signal observed at 1270 nm (see Figure 7b) was again assigned to the radiative decay of $O_2(^1\Delta_g)$. Analogous experiments carried out in deaerated tubes (see the procedure in the Experimental Section) containing the [(*phen*)Re(CO)$_3$Br]-doped SSO film (see Figure S2 in Supporting Information) showed no emission at 1270 nm. In addition, no signal was detected upon photoirradiation of the neat SSO film (Figure 7b), confirming that the observed infrared emission corresponds to $O_2(^1\Delta_g)$ and that the chemical species responsible for photosensitization is [(*phen*)Re(CO)$_3$Br]. Unequivocal confirmation of singlet oxygen generation by the doped film was obtained by measuring its characteristic emission spectrum centered at 1270 nm (Figure 7b inset).

Photooxidation of 9,10-Dimethylanthracene. To further explore the photosensitized formation of singlet oxygen from the samples of doped films, we performed photooxidation kinetic studies using DMA in MeCN, which is a well-known $O_2(^1\Delta_g)$ chemical trap. As mentioned in the Experimental Section, a [(*phen*)Re(CO)$_3$Br]-doped SSO film sample immersed in DMA solution was photoirradiated while the DMA absorption at 377 nm was simultaneously monitored. A control sample, in which the DMA solution was irradiated in the absence of film, was also run for comparison. The results of these experiments are shown in Figure 8.

During the first 5000 s of sample irradiation, the solution was purged with Ar, and the slight increase in the normalized concentration of DMA as a function of time observed for both samples can be ascribed to the MeCN evaporation. Upon

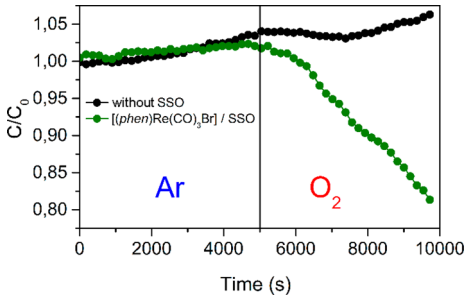

Figure 8. Oxidation of DMA in MeCN solution sensitized by the photoirradiation of the [(*phen*)Re(CO)$_3$Br]-doped SSO film (green line) with a blue LED (see the Experimental Section for details). A control sample without film (black line) is also shown for comparison. The DMA solutions (~8 × 10^{-5} M) were saturated with Ar and O_2 during 0−5000 s and 5000−10 000 s periods, respectively.

switching to O_2 purging (the 5000 to 10 000 s time interval), a significant decrease in the DMA concentration can be observed for the [(*phen*)Re(CO)$_3$Br]-doped SSO sample, which is associated with the photosensitized formation of $O_2(^1\Delta_g)$ by film irradiation and the subsequent reaction of DMA with $O_2(^1\Delta_g)$ to yield DMA−O_2. DMA consumption was not observed in a control sample without film (black trace), indicating that the self-photosensitization of DMA is insignificant under the employed conditions. The above results are consistent with the significant overlap of the emission spectrum of the blue LEDs with the absorption spectra of the [(*phen*)Re(CO)$_3$Br]-doped SSO film and with the lack of overlap with the spectra of DMA (see Figure S2 in the Supporting Information). These results further confirm the ability of the [(*phen*)Re(CO)$_3$Br]-doped SSO film to photosensitize the formation of $O_2(^1\Delta_g)$ under blue LED irradiation.

CONCLUSIONS

We have shown that [(*phen*)Re(CO)$_3$Br] embedded in a flexible SSO film maintains many photophysical properties and the ability to photosensitize the generation of $O_2(^1\Delta_g)$. The excellent properties of SSO films to homogeneously disperse opto-active molecular dopants within its polymer matrix are also demonstrated. These features, in addition to the great stability of the Re complex inside the polymer matrix, demonstrate that this approach can be useful for developing new hybrid materials composed of Re complexes and SSO building blocks with interesting and potentially useful optical properties. Furthermore, this composite can be the foundation for the formulation of microbial photoinactivating polymeric surfaces or the implementation of solid−liquid strategies for the photoinduced oxidation of organic compounds such as polyaromatic hydrocarbons in solution.

ASSOCIATED CONTENT

Supporting Information

Tables showing the bond distances and angles for the optimized geometry of [(*phen*)Re(CO)$_3$Br], calculated energies and composition of the two higher and lower unoccupied molecular orbitals for [(*phen*)Re(CO)$_3$Br], calculated emission transitions of [(*phen*)Re(CO)$_3$Br] in DCM and DMF, calculated energies and composition of the main molecular orbitals in [(*phen*)Re(CO)$_3$Br] emission transitions, and the luminescence lifetime of [(*phen*)Re(CO)$_3$Br in Ar-, air-, and O_2-saturated solution in DCM and DMF. Figures showing the

DOI: 10.1021/acs.jpcc.5b01990
J. Phys. Chem. C 2015, 119, 10148−10159

luminescence decay of O_2 generated by [(*phen*)Re(CO)$_3$Br] after irradiation and the overlapping of the absorption spectra of [(*phen*)Re(CO)$_3$Br] with LED emission and DMA absorption spectra. The Supporting Information is available free of charge on the ACS Publications website at DOI: 10.1021/acs.jpcc.5b01990. Crystallographic and structural details are provided in the CIF format. These data can be obtained free of charge from The Cambridge Crystallographic Data Centre via www.ccdc.cam.ac.uk/data_request/cif by requesting the deposit number CCDC-1030988.

AUTHOR INFORMATION

Corresponding Authors

*A.V. E-mail: andresvega@unab.cl. Tel: +56322845192.

*R.E.P. E-mail: rpalacios@exa.unrc.edu.ar. Tel: +543584676195.

Author Contributions

The manuscript was written through the contributions of all authors. R.M.S., M.L.G, M.C.-P., G.G., N.P., and A.V. carried out the experimental work. P.J. did all the computational work. M.L.G., R.E.P, A.V., and N.P. were responsible for project planning. Data analysis and interpretation were carried out by all the authors. N.P., A.V., G.G., and R.E.P. were primarily responsible for manuscript preparation. M.L.G., M.C.-P, and P.J. also contributed to the revision of the work. All authors have given approval to the final version of the manuscript.

Notes

The authors declare no competing financial interest.

ACKNOWLEDGMENTS

The authors gratefully acknowledge the partial financial support of Dirección de Investigación, Universidad Andres Bello, grant DI-111-12/R, Comisión Nacional de Ciencia y Tecnología, and grants FONDECYT 1120865 and ACE-03. M.C.P. acknowledges support from CONICYT 79130030. Additional financial support was given by grants from the following institutions: Agencia Nacional de Promoción Científica y Tecnológica (ANPCyT), Argentina (PICT 2691/11); Consejo Nacional de Investigaciones Científicas y Técnicas (CONICET), Argentina (PIP 11220090100839/10, 11220100100284/11); Secretaría de Ciencia y Técnica, UNRC Argentina; and Ministerio de Ciencia y Tecnología Córdoba, Argentina (PID 033/2010). A.V. is a member of Financiamiento Basal para Centros Científicos y Tecnológicos de Excelencia FB0807. M.L.G. and R.E.P. are permanent research staff of CONICET. R.M.S. thanks Secretaría de Ciencia y Técnica UNRC for an undergraduate research scholarship and CONICET for a Ph.D. scholarship. The authors thank PicoQuant for support provided to purchase the FluoTime 300 system currently operating at UNAB.

ABBREVIATIONS

DMF: *N*,*N*′-dimethylformamide; THF: tetrahydrofuran; MeCN: acetonitrile

REFERENCES

(1) Caspar, J. V.; Meyer, T. J. Application of the Energy Gap Law to Nonradiative, Excited-State Decay. *J. Phys. Chem.* **1983**, *87*, 952−957.

(2) Wallace, L.; Rillema, D. P. Ligand Substituent Effects on the Excited-State Properties of Rhenium(I) Tricarbonyl Complexes. *Abstr. Pap. Am. Chem. Soc.* **1993**, *205*, 396−INOR.

(3) Zipp, A. P.; Sacksteder, L.; Streich, J.; Cook, A.; Demas, J. N.; DeGraff, B. A. Luminescence of Rhenium(I) Complexes with Highly Sterically Hindered α-Diimine Ligands. *Inorg. Chem.* **1993**, *32*, 5629−5632.

(4) Cannizzo, A.; Blanco-Rodriguez, A. M.; El Nahhas, A.; Sebera, J.; Zalis, S.; Vlcek, A.; Chergui, M. Femtosecond Fluorescence and Intersystem Crossing in Rhenium(I) Carbonyl−Bipyridine Complexes. *J. Am. Chem. Soc.* **2008**, *130*, 8967−8974.

(5) Meyer, G. J. *Molecular Level Artificial Photosynthetic Materials*; Wiley: New York, 1996; Vol. *44*.

(6) Connick, W. B.; DiBilio, A. J.; Hill, M. G.; Winkler, J. R.; Gray, H. B. Tricarbonyl(1,10-Phenanthroline)(Imidazole)Rhenium(I): A Powerful Photo-oxidant for Investigations of Electron Tunneling in Proteins. *Inorg. Chim. Acta* **1995**, *240*, 169−173.

(7) Lo, K. K.-W.; Louie, M.-W.; Sze, K.-S.; Lau, J. S.-Y. Rhenium(I) Polypyridine Biotin Isothiocyanate Complexes as the First Luminescent Biotinylation Reagents: Synthesis, Photophysical Properties, Biological Labeling, Cytotoxicity, and Imaging Studies. *Inorg. Chem.* **2008**, *47*, 602−611.

(8) Oriskovich, T. A.; White, P. S.; Thorp, H. H. Luminescent Labels for Purine Nucleobases—Electronic Properties of Guanine Bound to Rhenium(I). *Inorg. Chem.* **1995**, *34*, 1629−1631.

(9) Salmain, M.; Gunn, M.; Gorfti, A.; Top, S.; Jaouen, G. Labeling of Proteins by Organometallic Complexes of Rhenium(I) — Synthesis and Biological Activity of the Conjugates. *Bioconjugate Chem.* **1993**, *4*, 425−433.

(10) Sundararajan, C.; et al. Synthesis and Characterization of Rhenium and Technetium-99m Labeled Insulin. *J. Med. Chem.* **2010**, *53*, 2612−2621.

(11) Bakir, M. The Optical Sensor Fac-Tricarbonyl-Chloro(Di-2-Pyridylmethanone P-Nitrophenylhydrazone)Rhenium(I) Dimethyl Sulfoxide Solvate. *Acta Crystallogr., Sect. C: Struct. Chem.* **2001**, *57*, 1371−1373.

(12) MacQueen, D. B.; Schanze, K. S. Cation-Controlled Photophysics in a Rhenium(I) Fluoroionophore. *J. Am. Chem. Soc.* **1991**, *113*, 6108−6110.

(13) Pelleteret, D.; Fletcher, N. C.; Doherty, A. P. Anion Detection Driven by a Surprising Internal Hydrogen-Bonding Association in a Dinuclear Rhenium(I) Complex. *Inorg. Chem.* **2007**, *46*, 4386−4388.

(14) Sun, S.-S.; Lees, A. J. Self-Assembly Triangular and Square Rhenium(I) Tricarbonyl Complexes: A Comprehensive Study of Their Preparation, Electrochemistry, Photophysics, Photochemistry, and Host−Guest Properties. *J. Am. Chem. Soc.* **2000**, *122*, 8956−8967.

(15) Takeda, H.; Ohashi, M.; Tani, T.; Ishitani, O.; Inagaki, S. Enhanced Photocatalysis of Rhenium(I) Complex by Light-Harvesting Periodic Mesoporous Organosilica. *Inorg. Chem.* **2010**, *49*, 4554−4559.

(16) Lundin, N. J.; Blackman, A. G.; Gordon, K. C.; Officer, D. L. Synthesis and Characterization of a Multicomponent Rhenium(I) Complex for Application as an Oled Dopant. *Angew. Chem., Int. Ed.* **2006**, *45*, 2582−2584.

(17) O'Regan, B.; Gratzel, M. A Low-Cost, High-Efficiency Solar Cell Based on Dye-Sensitized Colloidal Tio2 Films. *Nature* **1991**, *353*, 737−740.

(18) Tang, C. W.; VanSlyke, S. A. Organic Electroluminescent Diodes. *Appl. Phys. Lett.* **1987**, *51*, 913−915.

(19) Welter, S.; Brunner, K.; Hofstraat, J. W.; De Cola, L. Electroluminescent Device with Reversible Switching between Red and Green Emission. *Nature* **2003**, *421*, 54−57.

(20) Hieber, W.; Fuchs, H. Über Metallcarbonyle. Xxxix. Aminsubstituierte Rheniumcarbonyle. *Z. Anorg. Allg. Chem.* **1941**, *248*, 269−275.

(21) Wrighton, M.; Morse, D. L. Nature of the Lowest Excited State in Tricarbonylchloro-1,10-Phenanthrolinerhenium(I) and Related Complexes. *J. Am. Chem. Soc.* **1974**, *96*, 998−1003.

(22) Wagner, J. R.; Hendricker, D. G. Coordination of Mn(I) and Re(I) Carbonyls with Nitrogen Heterocyclic Ligands. *J. Inorg. Nucl. Chem.* **1975**, *37*, 1375−1379.

(23) Venegas, F.; Pizarro, N.; Vega, A. Structural and Photophysical Properties of a Mononuclear Re(I) Complex: P,N-{(C6h5)(2)-(C5h5n)P}Re(Co)(3)Br. *J. Chil. Chem. Soc.* **2011**, *56*, 823−826.

(24) Ragone, F.; Martinez Saavedra, H. H.; David Gara, P. M.; Ruiz, G. T.; Wolcan, E. Photosensitized Generation of Singlet Oxygen from Re(I) Complexes: A Photophysical Study Using Lioas and Luminescence Techniques. *J. Phys. Chem. A* **2013**, *117*, 4428−4435.
(25) Cerveau, G.; Corriu, R. J. P.; Framery, E. Influence of the Nature of the Catalyst on the Textural Properties of Organo-silsesquioxane Materials. *Polyhedron* **2000**, *19*, 307−313.
(26) Loy, D. A.; Shea, K. J. Bridged Polysilsesquioxanes. Highly Porous Hybrid Organic−Inorganic Materials. *Chem. Rev.* **1995**, *95*, 1431−1442.
(27) Shea, K. J.; Loy, D. A.; Webster, O. Arylsilsesquioxane Gels and Related Materials. New Hybrids of Organic and Inorganic Networks. *J. Am. Chem. Soc.* **1992**, *114*, 6700−6710.
(28) Fasce, D. P.; Williams, R. J. J.; Matejka, L.; Plestil, J.; Brus, J.; Serrano, B.; Cabanelas, J. C.; Baselga, J. Photoluminescence of Bridged Silsesquioxanes Containing Urea or Urethane Groups with Nano-structures Generated by the Competition between the Rates of Self-Assembly of Organic Domains and the Inorganic Polycondensation. *Macromolecules* **2006**, *39*, 3794−3801.
(29) Jain, V.; Khiterer, M.; Montazami, R.; Yochum, H. M.; Shea, K. J.; Heflin, J. R. High-Contrast Solid-State Electrochromic Devices of Viologen-Bridged Polysilsesquioxane Nanoparticles Fabricated by Layer-by-Layer Assembly. *ACS Appl. Mater. Interfaces* **2009**, *1*, 83−89.
(30) Gomez, M. L.; Fasce, D. P.; Williams, R. J. J.; Previtali, C. M.; Montejano, H. A. Transparent Polysilsesquioxane Films Obtained from Bridged Ureasil Precursors: Tunable Photoluminescence Emission in the Visible Region and Filtering of UV Radiation. *Macromol. Mater. Eng.* **2010**, *295*, 1042−1048.
(31) Gomez, M. L.; Fasce, D. P.; Williams, R. J. J.; Previtali, C. M.; Matejka, L.; Plestil, J.; Brus, J. Tuning the Photoluminescence of Silsesquioxanes with Short Substituted Urea Bridges. *Macromol. Chem. Phys.* **2008**, *209*, 634−642.
(32) Gómez, M. L.; Fasce, D. P.; Williams, R. J. J.; Montejano, H. A.; Previtali, C. M. Photoluminescence of Bridged Polysilsesquioxanes Containing Urea Groups: Doping with Safranine-O to Generate Red-Light Emission. *J. Polym. Sci., Part B: Polym. Phys.* **2008**, *46*, 289−296.
(33) Nobre, S. S.; Brites, C. D. S.; Ferreira, R. A. S.; de Zea Bermudez, V.; Carcel, C.; Moreau, J. J. E.; Rocha, J.; Wong Chi Man, M.; Carlos, L. D. Photoluminescence of Eu(III)-Doped Lamellar Bridged Silsesquioxanes Self-Templated through a Hydrogen Bonding Array. *J. Mater. Chem.* **2008**, *18*, 4172−4182.
(34) Graffion, J.; Cojocariu, A. M.; Cattoen, X.; Ferreira, R. A. S.; Fernandes, V. R.; Andre, P. S.; Carlos, L. D.; Wong Chi Man, M.; Bartlett, J. R. Luminescent Coatings from Bipyridine-Based Bridged Silsesquioxanes Containing Eu3+ and Tb3+ Salts. *J. Mater. Chem.* **2012**, *22*, 13279−13285.
(35) Gómez, M. L.; Hoppe, C. E.; Zucchi, I. A.; Williams, R. J. J.; Giannotti, M. I.; López-Quintela, M. A. Hierarchical Assemblies of Gold Nanoparticles at the Surface of a Film Formed by a Bridged Silsesquioxane Containing Pendant Dodecyl Chains. *Langmuir* **2008**, *25*, 1210−1217.
(36) Gómez, M.; dell'Erba, I.; Chesta, C.; Hoppe, C.; Williams, R. J. Dispersion of Gold Dodecanethiolate in a Silsesquioxane Film with Pendant Dodecyl Chains: From Photoluminescent Materials to Gold Nanocomposites. *J. Mater. Sci.* **2013**, *48*, 8559−8565.
(37) Gómez, M. L.; Hoppe, C. E.; Williams, R. J. J. In Situ Generation of Silver Microstructures by Thermal Decomposition of Silver N-Dodecanethiolate Dispersed in an Organic−Inorganic Hybrid Coating. *Mater. Chem. Phys.* **2011**, *130*, 519−523.
(38) Alvarez, M. G.; Gómez, M. L.; Mora, S. J.; Milanesio, M. E.; Durantini, E. N. Photodynamic Inactivation of Candida Albicans Using Bridged Polysilsesquioxane Films Doped with Porphyrin. *Bioorg. Med. Chem.* **2012**, *20*, 4032−4039.
(39) Bonnett, R.; Buckley, D. G.; Burrow, T.; Galia, A. B. B.; Saville, B.; Songca, S. P. Photobactericidal Materials Based on Porphyrins and Phthalocyanines. *J. Mater. Chem.* **1993**, *3*, 323−324.
(40) Kenley, R. A.; Kirshen, N. A.; Mill, T. Photooxidation of Di-N-Butyl Sulfide Using Sensitizers Immobilized in Polymer Films. *Macromolecules* **1980**, *13*, 808−815.
(41) McCluskey, D. M.; Smith, T. N.; Madasu, P. K.; Coumbe, C. E.; Mackey, M. A.; Fulmer, P. A.; Wynne, J. H.; Stevenson, S.; Phillips, J. P. Evidence for Singlet-Oxygen Generation and Biocidal Activity in Photoresponsive Metallic Nitride Fullerene−Polymer Adhesive Films. *ACS Appl. Mater. Interfaces* **2009**, *1*, 882−887.
(42) *SAINTPLUS*, V6.22; Bruker AXS Inc.: Madison, WI.
(43) Sheldrick, G. M.; S, N. V.. *SHELXL*;Bruker AXS Inc.: Madison, WI, 2000.
(44) *SADABS*, V2.05; Bruker AXS Inc.: Madison, WI.
(45) Crosby, G. A.; Demas, J. N. Measurement of Photo-luminescence Quantum Yields. Review. *J. Phys. Chem.* **1971**, *75*, 991−1024.
(46) Wilkinson, F.; Helman, W. P.; Ross, A. B. Quantum Yields for the Photosensitized Formation of the Lowest Electronically Excited Singlet State of Molecular Oxygen in Solution. *J. Phys. Chem. Ref. Data* **1993**, *22*, 113−262.
(47) Schmidt, R. The Effect of Solvent Polarity on the Balance between Charge Transfer and Non-Charge Transfer Pathways in the Sensitization of Singlet Oxygen by $\pi\pi^*$ Triplet States. *J. Phys. Chem. A* **2006**, *110*, 5990−5997.
(48) Gunther, G.; Lemp, E.; Zanocco, A. L. On the Use of 9,10-Dimethylanthracene as Chemical Rate Constant Actinometer in Singlet Molecular Oxygen Reactions. *Bol. Soc. Chil. Quim.* **2000**, *45*, 637−644.
(49) Schmidt, R.; Schaffner, K.; Trost, W.; Brauer, H. D. Wavelength-Dependent and Dual Photochemistry of the Endoperoxides of Anthracene and 9,10-Dimethylanthracene. *J. Phys. Chem.* **1984**, *88*, 956−958.
(50) Frisch, M. J.; Trucks, G. W.; Schlegel, H. B.; Scuseria, G. E.; Robb, M. A.; Cheeseman, J. R.; Scalmani, G.; Barone, V.; Mennucci, B.; Petersson, G. A.; Nakatsuji, H.; et al. *Gaussian 09*; Gaussian, Inc.: Wallingford, CT, 2009.
(51) Becke, A. Density-Functional Exchange-Energy Approximation with Correct Asymptotic Behavior. *Phys. Rev. A: At., Mol., Opt. Phys.* **1988**, *38*, 3098−3100.
(52) Lee, C.; Yang, W.; Parr, R. Development of the Colle−Salvetti Correlation Energy Formula into a Functional of the Electron Density. *Phys. Rev. B: Condens. Matter Mater. Phys.* **1988**, *37*, 785−789.
(53) Hay, P. J.; Wadt, W. R. Ab Initio Effective Core Potentials for Molecular Calculations. Potentials for K to Au Including the Outermost Core Orbitals. *J. Chem. Phys.* **1985**, *82*, 299−310.
(54) Miertuš, S.; Scrocco, E.; Tomasi, J. Electrostatic Interaction of a Solute with a Continuum. A Direct Utilizaion of Ab Initio Molecular Potentials for the Prevision of Solvent Effects. *Chem. Phys.* **1981**, *55*, 117−129.
(55) Lakowicz, J. R. *Principles of Fluorescence Spectroscopy*; Springer: New York, 2006.
(56) Ramakrishnan, S.; Palaniandavar, M. Mixed-Ligand Copper(II) Complexes of Dipicolylamine and 1,10-Phenanthrolines: The Role of Diimines in the Interaction of the Complexes with DNA. *J. Chem. Sci.* **2005**, *117*, 179−186.
(57) Vallee, B. L.; Rupley, J. A.; Coombs, T. L.; Neurath, H. The Role of Zinc in Carboxypeptidase. *J. Biol. Chem.* **1960**, *235*, 64−69.
(58) El Nahhas, A.; et al. Ultrafast Excited-State Dynamics of Rhenium(I) Photosensitizers [Re(Cl)(Co)3(*N*,*N*)] and [Re-(Imidazole)(Co)3(*N*,*N*)]$^+$: Diimine Effects. *Inorg. Chem.* **2011**, *50*, 2932−2943.
(59) Si, Z.; Li, X.; Li, X.; Zhang, H. Synthesis, Photophysical Properties, and Theoretical Studies on Pyrrole-Containing Bromo Re(I) Complex. *J. Organomet. Chem.* **2009**, *694*, 3742−3748.
(60) Martinez Saavedra, H. H.; Ragone, F.; Ruiz, G. T.; Gara, P. M. D.; Wolcan, E. Solvent Dependent Switching of 3MLLCT and 1Il Luminescent States in [ClRe(CO)3(bathocuproinedisulfonate)]$^{2-}$: Spectroscopic and Computational Study. *J. Phys. Chem. A* **2014**, *118* (41), 9661−9674.
(61) Caspar, J. V.; Meyer, T. J. Photochemistry of Tris(2,2′-Bipyridine)Ruthenium(2+) Ion (Ru(Bpy)32+). Solvent Effects. *J. Am. Chem. Soc.* **1983**, *105*, 5583−5590.

DOI: 10.1021/acs.jpcc.5b01990
J. Phys. Chem. C 2015, 119, 10148−10159

(62) Nahhas, A. E.; Cannizzo, A.; Mourik, F. v.; Blanco-Rodríguez, A. M.; Záliš, S.; Vlček, J. A.; Chergui, M. Ultrafast Excited-State Dynamics of [Re(L)(Co)3(Bpy)]N Complexes: Involvement of the Solvent. *J. Phys. Chem. A* **2010**, *114*, 6361−6369.
(63) Balk, R. W.; Stufkens, D. J.; Oskam, A. Characterization of Metal-to-Ligand Charge Transfer and Intraligand Transitions of Fac-[Re(Co)3l(X)] Complexes [L = Di-Imine; X = Halide or Mn(Co)5] and Explanation of the Photochemistry of [Re(Co)3l{Mn(Co)5}] Using the Resonance Raman Effect. *J. Chem. Soc., Dalton Trans.* **1981**, 1124−1133.
(64) Kotch, T. G., et al. *Luminescence Rigidochromism of Fac-Cire(Co)[3](4,7-Ph[2]Phen) (4,7-Ph[2]Phen = 4,7-Diphenyl-1,10-Phenantroline) as a Spectroscopic Probe in Monitoring Polymerization of Photosensitive Thin Films*; American Chemical Society: Washington, DC, 1993; Vol. *32*.
(65) Wallace, L.; Woods, C.; Rillema, D. P. Structure and Luminescence Properties of Re(4,7-Dimethyl-1,10-Phenanthroline)-(Co)(3)Py (+) in a Solid Matrix. *Inorg. Chem.* **1995**, *34*, 2875−2882.
(66) Lin, S. H. Rate of Interconversion of Electronic and Vibrational Energy. *J. Chem. Phys.* **1966**, *44*, 3759−3767.
(67) Sacksteder, L.; Zipp, A. P.; Brown, E. A.; Streich, J.; Demas, J. N.; Degraff, B. A. Luminescence Studies of Pyridine Alpha-Diimine Rhenium(I) Tricarbonyl Complexes. *Inorg. Chem.* **1990**, *29*, 4335−4340.
(68) Leasure, R. M.; Sacksteder, L.; Nesselrodt, D.; Reitz, G. A.; Demas, J. N.; DeGraff, B. A. Excited-State Acid−Base Chemistry of (α-Diimine)Cyanotricarbonylrhenium(I) Complexes. *Inorg. Chem.* **1991**, *30*, 3722−3728.
(69) Hurst, J. R.; McDonald, J. D.; Schuster, G. B. Lifetime of Singlet Oxygen in Solution Directly Determined by Laser Spectroscopy. *J. Am. Chem. Soc.* **1982**, *104*, 2065−2067.
(70) Ragone, F.; Martinzes Saavedra, H. H.; Gara, P. M. D.; Ruiz, G. T.; Wolcan, E. Photosensitized Generation of Singlet Oxygen from Re(I) Complexes: A Photophysical Study Using Lioas and Luminescence Techniques. *J. Phys. Chem. A* **2013**, *117*, 4428−4435.
(71) Abdel-Shafi, A. A.; Bourdelande, J. L.; Ali, S. S. Photosensitized Generation of Singlet Oxygen from Rhenium(I) and Iridium(III) Complexes. *Dalton Trans.* **2007**, 2510−2516.

DOI: 10.1021/acs.jpcc.5b01990
J. Phys. Chem. C 2015, 119, 10148−10159